

Precision measurement of single atoms strongly coupled to the higher-order transverse modes of a high-finesse optical cavity

Jinjin Du, Wenfang Li, Ruijuan Wen, Gang Li, and Tiancai Zhang

Citation: *Appl. Phys. Lett.* **103**, 083117 (2013); doi: 10.1063/1.4819228

View online: <http://dx.doi.org/10.1063/1.4819228>

View Table of Contents: <http://apl.aip.org/resource/1/APPLAB/v103/i8>

Published by the AIP Publishing LLC.

Additional information on *Appl. Phys. Lett.*

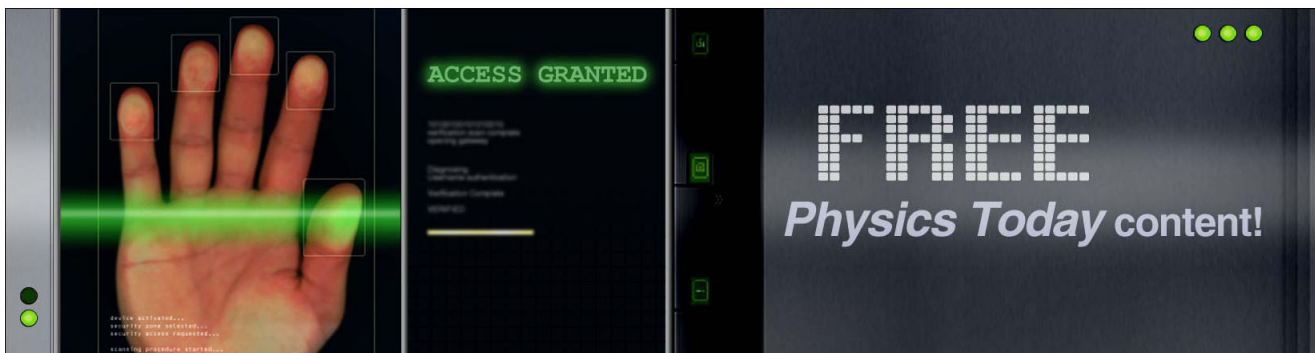
Journal Homepage: <http://apl.aip.org/>

Journal Information: http://apl.aip.org/about/about_the_journal

Top downloads: http://apl.aip.org/features/most_downloaded

Information for Authors: <http://apl.aip.org/authors>

ADVERTISEMENT



Precision measurement of single atoms strongly coupled to the higher-order transverse modes of a high-finesse optical cavity

Jinjin Du, Wenfang Li, Ruijuan Wen, Gang Li, and Tiancai Zhang^{a)}

State Key Laboratory of Quantum Optics and Quantum Optics Devices, Institute of Opto-Electronics, Shanxi University, Taiyuan 030006, China

(Received 15 July 2013; accepted 11 August 2013; published online 23 August 2013)

We have experimentally demonstrated the strong coupling between single atoms and the higher-order Hermite-Gaussian transverse modes in a high-finesse optical microcavity. Compared to the usual low-order symmetric transverse modes, multiple lobes and the asymmetric spatial pattern of the titled modes provide more information about the motion of single atoms in the cavity. The motional information can be extracted from the measured transmission spectra, which includes the velocities and the positions of the atoms in vertical and off-axis directions. The scheme has great potential in time-resolved atom-cavity microscopy and in tracking the three-dimensional single atom trajectory in real time. © 2013 AIP Publishing LLC. [<http://dx.doi.org/10.1063/1.4819228>]

Manipulation and measurement of single atoms are important for studying the atom-photon interaction,¹ quantum state preparation,^{2,3} quantum entanglement,^{4,5} and fundamental quantum physics.^{6,7} The deterministic control and measurement of individual atoms are also the preconditions for quantum information processing based on atoms and photons.⁸ The main difficulty in implementing quantum information processing and communication protocols in present demonstration experiments is actually the enormous complexity required to obtain full control over both atoms and photons at the single particle level.⁹

However, the size of optical trap for single atoms is normally on the micrometer scale and is basically limited by the diffraction of the trap beam; thus, the spatial confinement is about four orders of magnitude larger than the size of the atom itself. The scattering section of single atoms is rather small, which causes difficulty in sensing the atom individually in free space. With the very complex configurations of atom control^{10,11} and some new techniques, such as surface plasmonics,^{12–15} one may break through the limitation of the trapping size for better confinement of an atom and reach sub-micrometer scale. Nevertheless, seeking an approach to confine and track the atom's position with high resolution is still a challenge. Cavity quantum electrodynamics (QED) provides an enhanced interaction between single atoms and the cavity. The strongly coupled cavity QED system enables us to track and even control the position of single atoms in real time by feedback.^{16–19} With the symmetric TEM_{10} cavity modes,²⁰ trajectory of single atoms can be determined with an improved spatial resolution. In our previous work, we have demonstrated the elimination of the degenerate trajectory of a single atom by the tilted TEM_{10} mode.²¹ Taking this forward, one may expect that by employing even higher-order cavity modes, further improvement of trajectory measurement could be realized, provided that the atom-cavity interaction is still in strong coupling regime.

In this paper, we have demonstrated in experiment the strong coupling between single atoms and higher-order Hermite-Gaussian modes TEM_{m0} up to $m=3$ inside a high-finesse optical microcavity. The axis of the nodal lines of the higher-order modes are inclined 45° to the vertical direction. The transmission spectra for atom coupling to these cavity modes are measured in experiment. We have theoretically analysed the process and the corresponding atomic motional information is extracted. The experimental limitation of single atom sensing for even higher transverse modes is discussed.

The experimental system layout is shown in Fig. 1. A Fabry-Pérot cavity consists of two super-polished spherical mirrors with a radius of curvature of 100 mm and an end-diameter of 1 mm. The waist of intra-cavity TEM_{00} mode is $\omega_0 = 23.8 \mu\text{m}$. The finesse of the cavity is 3.3×10^5 and for TEM_{00} mode we have $(g_0, \kappa, \gamma) = 2\pi \times (23.9, 2.6, 2.6)\text{MHz}$, where g_0 is the maximum coupling efficiency (the atom is located in the antinodes) between cavity TEM_{00} mode and atoms, and κ, γ are the cavity decay rate and atom decay rate, respectively. A weak probe laser beam at wavelength of 852 nm is tuned close to the transition of cesium D_2 line: $6^2S_{1/2}, F=4 \rightarrow 6^2P_{3/2}, F=5$. We use an external cavity

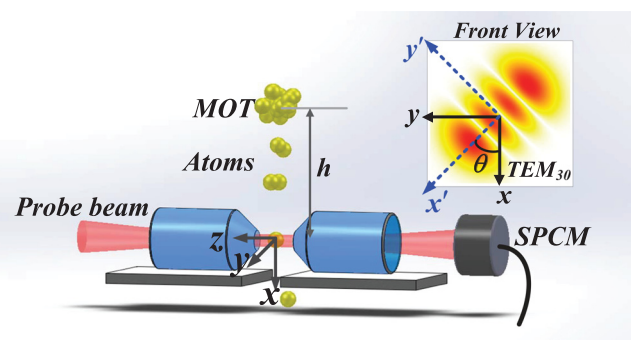


FIG. 1. Atom-cavity coupling system. The atoms are trapped in a MOT and dropped through the high finesse optical cavity. The transmission of the cavity is measured by single photon counting module. The top-right denotes a tilted three-order mode of the cavity from the front view (viewing along z axis direction) and a rotating frame coordinate transformation is illustrated.

^{a)} Author to whom correspondence should be addressed. Electronic mail: tczhang@sxu.edu.cn

diode laser (ECDL) working at 828 nm as the cavity locking beam to keep the stability of cavity length. The details of the experimental setup have been introduced in our previous works.²²

The experiment is performed in the following sequences: roughly 10^5 atoms are initially accumulated in a magneto-optical trap (MOT) which is located about 6 mm above the center of the cavity. After a polarization gradient cooling phase, the trapping laser beams and magnetic field are switched off, and the atoms fall freely under gravity. Some of the atoms will transit through the cavity mode and induce a change in the cavity transmission field due to the strong coupling. We deliberately misaligned the probe beam slightly to enhance the coupling efficiency of the higher-order transverse cavity mode, making one of

higher-order modes resonant to the cavity by choosing proper cavity length. The transmission spectra of the cavity are measured by single-photon-counting module (SPCM-AQR-15, PerkinElmer) with total photon detection efficiency, including the cavity escape efficiency, the propagation efficiency, and the detection efficiency, $\eta = 0.075$.²³

The reference frame and the corresponding coordinates are shown in Fig. 1. The origin of the frame is in the center of the cavity and the z axis is along cavity mode. The process that the atom transits the tilted cavity mode in strong coupling regime has been discussed.²¹ In the case of weak excitation conditions (the average photon number $n \approx 1$), the cavity transmission is reduced to a two-dimensional expression near the antinode of the cavity field (the frame origin $z \approx 0$):

$$T(x, y) = \frac{\kappa^2(\gamma^2 + \Delta_{pa}^2)}{[g_{eff}(x, y)^2 - \Delta_{pa}^2 + \Delta_{ca}\Delta_{pa} + \gamma\kappa]^2 + (\kappa\Delta_{pa} + \gamma\Delta_{pa} - \gamma\Delta_{ca})^2}, \quad (1)$$

where T is already normalized to the transmission of the empty cavity. $\Delta_{pa} = \omega_{probe} - \omega_{atom}$ denotes the detuning between probe light and atomic transition, and $\Delta_{ca} = \omega_{cavity} - \omega_{atom}$ is the detuning between cavity and atom. The effective coupling efficiency g_{eff} for arbitrary Hermite-Gaussian transverse modes is determined by the actual position of the atom in the cavity mode, i.e., $g_{eff}(x, y) = g_0\Psi_{m,n}(x', y')/\Psi_{0,0}(0, 0)$, where g_0 is the maximum coupling efficiency in the TEM_{00} mode where the atom locates in the antinodes. Here, we have reasonably assumed that the atom trajectories in the cavity are straight lines along the vertical direction, as was discussed in Ref. 24.

In practice, there is an angle of θ between the nodal lines of TEM_{mn} modes and x axis, which can be measured experimentally. Thus, rotating frame coordinate transformation $x' = x \cos \theta + y \sin \theta$, $y' = -x \sin \theta + y \cos \theta$ could be used to obtain the transmission spectra. The mode field distribution of TEM_{mn} mode thus could be expressed as

$$\Psi_{m,n}(x', y') = C_{m,n} \exp\left(-\frac{x'^2 + y'^2}{\omega_0^2}\right) H_m\left(\frac{\sqrt{2}x'}{\omega_0}\right) H_n\left(\frac{\sqrt{2}y'}{\omega_0}\right), \quad (2)$$

where $C_{m,n} = (2^m 2^n m! n!)^{-1/2} (\omega_0^2 \pi/2)^{-1/2}$, and $H_{m,n}$ represent the corresponding Hermite polynomials in the order of m and n . ω_0 is the waist of the mode which is determined by the radius of mirror curvature and the cavity length. The eigen-frequencies of TEM_{mn} modes are

$$\omega_{m,n,q} = \left[q + \frac{n+m+1}{\pi} \arccos(\sqrt{\zeta_1 \zeta_2}) \right] \frac{\pi c}{L}, \quad (3)$$

where q is the longitudinal mode index along the cavity z -axis, $\zeta_{1,2} = 1 - L/R_{1,2}$ with L the length of the cavity and $R_{1,2}$ the radius of curvature of the input and output mirrors, respectively. Equation (3) shows that for an axial-symmetric F-P cavity, the higher-order transverse modes with identical

indices q and $N = m + n$ are actually degenerate in resonance frequencies. Fortunately due to the deformation of the mirrors, there are about tens of MHz of transverse mode spacing in our experiment and we can then distinguish each mode clearly. Recently, Kim *et al.* reported a method²⁵ to remove and separate the degeneracy frequencies in a controlled way. The deformation is inherent in the mirror polishing, the coating, and glue processing. One can obtain the different high-order degenerated transverse modes by scanning either the cavity length or the probe beam frequency. Fig. 2 shows the spectra of a set of well-separated higher-order transverse modes. The insets show the details of each set of high order modes. The transmissions around the cavity resonances and the mode spacing can be measured precisely by modulated RF sidebands which are added on the probe beam. Fig. 2 also shows the images (see the right top) of the different transverse modes taken by a CCD camera when the mode is resonant to the cavity separately.

Since the mode volume increases as the order of modes increases, the coupling between single atoms and the cavity become weaker. The maximum coupling efficiency $g_{max}(m, n)$ versus the transverse mode orders $m + n$ is shown

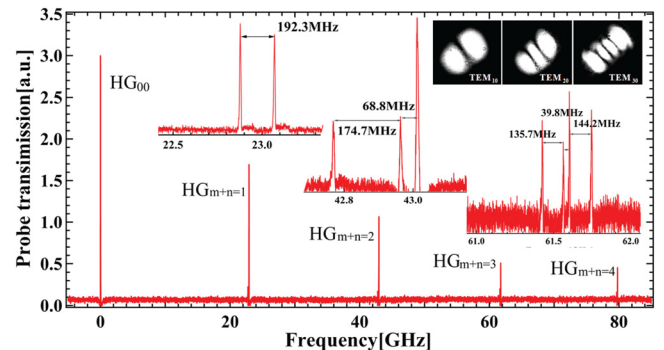


FIG. 2. Cavity transmission on resonance when the cavity length is scanned. The inset shows spacing of different higher modes for the same values $m + n$ and the corresponding images viewed by CCD.

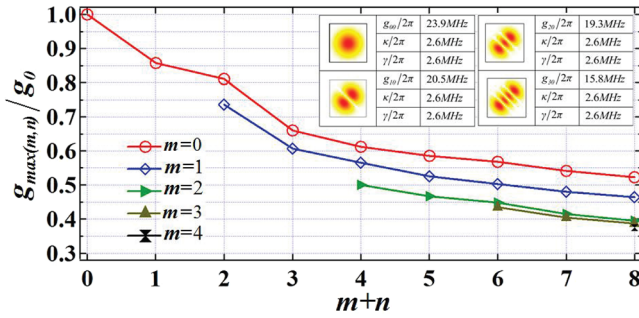


FIG. 3. Normalized single-photon coupling between atom and cavity as a function of the mode orders $m+n$. $g_{\max(m,n)}$ is the maximum coupling between the atom and the corresponding TEM_{mn} mode. g_0 is the maximum coupling efficiency in the TEM_{00} mode.

in Fig. 3. It can be seen that in a wide range of mode order, the system is in the strong coupling regime, i.e., $g_{\max}(m, n)$ is much larger than γ and κ .

The cavity transmissions given by Eqs. (1) and (2) for a 45° tilted mode are shown in Fig. 4 when atoms go into the cavity mode in different positions along the y axis. Other parameters we used for the simulation are the detuning of cavity and atom $\Delta_{ca} = 0$ MHz, the detuning of probe laser and atom $\Delta_{pa} = 0$ MHz, and the waist of the cavity $\omega_0 = 23.8 \mu\text{m}$. From left to right, Figs. 4(a)–4(c) correspond to Hermite-Gaussian transverse modes TEM_{m0} with $m=1$ to 3. As the mode order increases, the number of mode nodes also increases, which results in more complex patterns of the spectra. In principle, more lobes in the higher order modes provide more turning points where the coupling reaches maximum or minimum when an atom passes each lobe. The size of each lobe is smaller than that of the TEM_{00} mode which implies that higher order modes with more lobes can provide more fine spatial information of an atom, as it is in a more confined space. This means that when we use higher order transverse modes, in a similar experimental situation of using lower modes, the transmission spectra can provide the capability of obtaining the trajectory of the single atom with higher spatial resolution. Of course, the tilted intra-cavity mode with asymmetric spatial pattern, as a preceding condition, guarantees the unique determination of the single atom trajectory, as was discussed in Ref. 21.

A well-stabilized home-made laser is used as the probe beam through which the transmission spectra of the single atom transits is recorded when the intra-cavity mode is locked in TEM_{10} , TEM_{20} , and TEM_{30} , respectively. The results are shown in Fig. 5, where the intra-cavity average photon number is about 1, corresponding to 1.8 pW of output beam power from the cavity. The red diamonds are the experimental data and the black lines are the fittings according to Eqs. (1) and (2). The trajectory information shown on the

top-right in each graph is extracted directly from the spectra fitting, which includes the off-axis position y , the vertical velocity v , and their corresponding uncertainties. The information on atomic position and velocity in the cavity mode can be obtained from the transmission spectra. The extent of trajectory change is sensitive to the position of the atom inside the cavity and the order of the modes. In the similar experimental condition (it is difficult to perform the atom transits every time in the exact same place because the atoms fall down under gravity and its location is uncontrollable.), the statistical uncertainty of about $0.33 \mu\text{m}$, $0.28 \mu\text{m}$, and $0.26 \mu\text{m}$ for TEM_{10} , TEM_{20} , and TEM_{30} modes are obtained in off-axis direction (axis y), respectively, and the corresponding statistical uncertainty in vertical direction (x -direction) is $4.02 \mu\text{m}$, $3.06 \mu\text{m}$, and $1.95 \mu\text{m}$ within $10 \mu\text{s}$, respectively. From the results, the following main points can be established:

- i) On the whole, the recorded experimental transmission spectra agree with the theoretical fittings given by Fig. 4.
- ii) For the same order of mode, the uncertainty of y strongly depends on the exact position where the atom falls. The closer the trajectory to the center of the antinode ($y=0$), the lower the uncertainty that can be obtained. When an atom transits at a position far away from the mode center, the signal-to-noise ratio (SNR) of the spectrum becomes low and the uncertainty increases.
- iii) The records show that optimal uncertainty is about $0.26 \mu\text{m}$ which is obtained for $y=0.53 \mu\text{m}$ by using TEM_{30} mode. When we use TEM_{20} in place of TEM_{10} mode, the obtained uncertainties are substantially improved, but for even higher order mode TEM_{30} , further improvement is not obvious. The obvious restriction is the signal-to-noise ratio of the spectrum which is deteriorating as the atom-cavity coupling becomes relatively weaker for higher order modes, see Fig. 3.
- iv) The uncertainty of velocity measurement in the vertical direction (x direction) is also substantially reduced by using a higher order cavity mode, which is directly due to the multiple nodal points. The best spatial resolution in the vertical direction (axis x) is about $1.95 \mu\text{m}$ within $10 \mu\text{s}$ of integrate time, which is again obtained by TEM_{30} . We also see that the highest accuracy by TEM_{30} mode is obtained when the atom velocity is about 2 times slower than in other data, which means that by using a slower atom sample, we could increase the atom-cavity interaction time and improve our measurement accuracy further. In principle, a slower atom, by using an additional deceleration phase or other atom feeding method (such as atom convey belt by 1D optical lattice), could be used to enhance the measurement accuracy further.

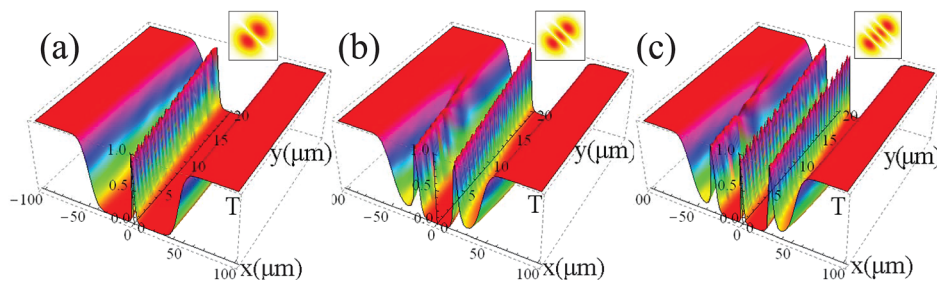


FIG. 4. Cavity transmission spectra according to Eqs. (1) and (2) as functions of the coordinates x and y for different higher order transverse modes. The parameters of our experimental system are as follows: $(g_0, \kappa, \gamma) = 2\pi \times (23.9, 2.6, 2.6)$ MHz, $\Delta_{ca} = \Delta_{pa} = 0$ MHz, and the waist of the cavity $\omega_0 = 23.8 \mu\text{m}$ for the probe beam.

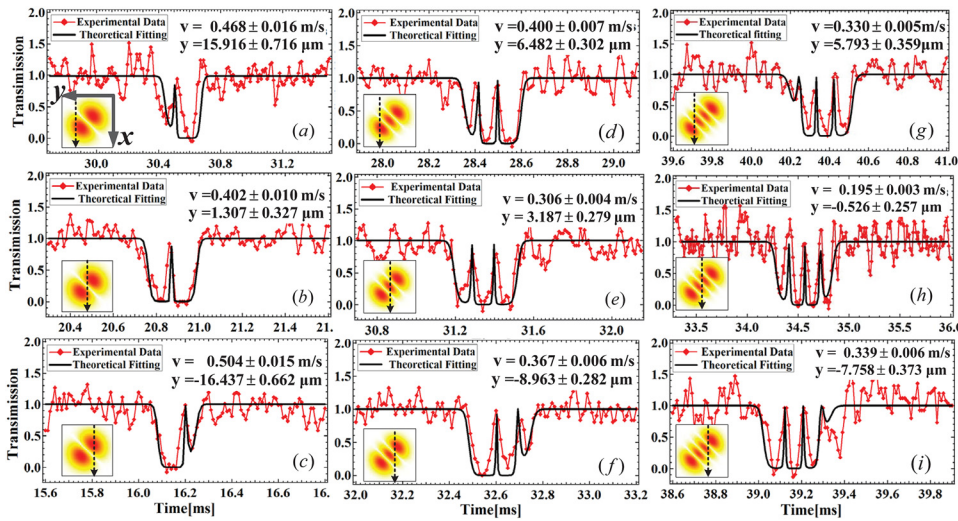


FIG. 5. Cavity transmission spectra of a single atom coupled to different tilted TEM_{m0} ($m = 1, 2, 3$) modes of a high-finesse optical cavity. The red diamonds are the experimental data and the black solid curves are theoretical fittings according to Eqs. (1) and (2). The insets at bottom-left show where the atom passes (see the black dotted arrow). The weak probe laser is resonant to both the cavity mode and the atom. The corresponding fitting results of the atom position and its uncertainties are shown in each graph.

The motional information of single atoms in higher-order transverse modes in the high finesse optical cavity can be determined with rather low uncertainty. The actual uncertainty mainly relies on the signal-to-noise ratio which is influenced by the following aspects: the location of the atom, the order of transverse mode and the noise from the probe beam, and the locking system. At this moment, we cannot control the location where the atom passes. We have to do the trade off for choosing the proper order of the transverse mode since higher order modes imply low coupling coefficient and poor signal-to-noise ratio. The imperfect locking system in the cavity QED experiment indeed induces some technical noise, including imperfection of the feedback control system for cavity length stabilization, the frequency chain system,²⁶ the cavity drift from the temperature change, and the noise from the probe laser. If all these noises were killed, we would have used even higher order of modes TEM_{m0} ($m > 3$) and the advantages of using higher order mode to sense the single atom would be more prominent. Right now, we have demonstrated that multiple lobes of higher order transverse modes do improve the measurement precision of a single atom's position and velocity.

In summary, we have demonstrated the strong coupling between a single atom and the tilted higher-order transverse modes up to TEM_{30} inside a high-finesse optical cavity. The position of single atom and its velocity are measured by the cavity transmission spectra with high precision. The experimental results are consistent with the theory. Multiple lobes of the asymmetric spatial pattern of the higher-order transverse modes can indeed improve the measurement of a single atom position in both transverse directions. The results show that the best spatial resolutions of $1.95 \mu\text{m}$ in vertical direction (axis x) within $10 \mu\text{s}$ and $0.26 \mu\text{m}$ for off-axis direction (axis y) are obtained when an atom freely falls and strongly coupled to TEM_{30} mode. The signal-to-noise ratio is determined by the coupling coefficient and the noise which results from the fluctuation of various technical noises and the Poissonian photon noise. If the collection efficiency can be improved or the speed at which the atom enters into the cavity can be reduced, more photons emitted by the atom can be detected and the signal-to-noise ratio should be higher. Multiple longitudinal modes interacting with single atoms in

the cavity based on this system are interesting. In that case, the dipole traps with multiple colors inside the cavity will be built up, which can provide further confinement for single atom.^{10,11} By joint using the method here we provided, choosing the proper frequencies of multiple modes and the feedback control techniques,²⁷ the system shows great potential for further increasing the spatial resolution of single atoms.

The work was supported by the Major State Basic Research Development Program of China (Grant No. 2012CB921601) and the National Natural Science Foundation of China (Grant Nos. 11125418, 61227902, 61275210, 11204165, 61121064).

- ¹J. McKeever, A. Boca, A. D. Boozer, R. Miller, J. R. Buck, A. Kuzmich, and H. J. Kimble, *Science* **303**, 1992 (2004).
- ²A. Kuhn, M. Hennrich, and G. Rempe, *Phys. Rev. Lett.* **89**, 067901 (2002).
- ³H. J. Kimble, *Phys. Rev. Lett.* **90**, 249801 (2003).
- ⁴T. Wilk, S. C. Webster, A. Kuhn, and G. Rempe, *Science* **317**, 488 (2007).
- ⁵B. Weber, H. P. Specht, T. Müller, J. Bochmann, M. Mücke, D. L. Moehring, and G. Rempe, *Phys. Rev. Lett.* **102**, 030501 (2009).
- ⁶N. Sangouard, C. Simon, J. Minář, H. Zbinden, H. de Riedmatten, and N. Gisin, *Phys. Rev. A* **76**, 050301(R) (2007).
- ⁷R. Alleaume, F. Treussart, G. Messin, Y. Dumeige, J.-F. Roch, A. Beveratos, R. Brouri-Tualle, J.-P. Poizat, and P. Grangier, *New J. Phys.* **6**, 92 (2004).
- ⁸C. Monroe, *Nature* **416**, 238 (2002).
- ⁹P. Zoller, Th. Beth, D. Binosi, R. Blatt, H. Briegel, D. Bruss, T. Calarco, J. I. Cirac, D. Deutsch, J. Eisert, A. Ekert, C. Fabre, N. Gisin, P. Grangiere, M. Grassl, S. Haroche, A. Imamoglu, A. Karlson, J. Kempe, L. Kouwenhoven, S. Kröll, G. Leuchs, M. Lewenstein, D. Loss, N. Lütkenhaus, S. Massar, J. E. Mooij, M. B. Plenio, E. Polzik, S. Popescu, G. Rempe, A. Sergienko, D. Suter, J. Twamley, G. Wendin, R. Werner, A. Winter, J. Wrachtrup, and A. Zeilinger, *Eur. Phys. J. D* **36**, 203 (2005).
- ¹⁰P. Xu, X. D. He, J. Wang, and M. S. Zhan, *Opt. Lett.* **35**, 2164 (2010).
- ¹¹G. Li, S. Zhang, L. Isenhower, K. Maller, and M. Saffman, *Opt. Lett.* **37**, 851 (2012).
- ¹²D. E. Chang, J. D. Thompson, H. Park, V. Vuletić, A. S. Zibrov, P. Zoller, and M. D. Lukin, *Phys. Rev. Lett.* **103**, 123004 (2009).
- ¹³C. Stehle, H. Bender, C. Zimmermann, D. Kern, M. Fleischer, and S. Slama, *Nat. Photonics* **5**, 494 (2011).
- ¹⁴Y. Gu, L. J. Wang, P. Ren, J. X. Zhang, T. C. Zhang, O. J. F. Martin, and Q. H. Gong, *Nano Lett.* **12**, 2488 (2012).
- ¹⁵J. D. Thompson, T. G. Tiecke, N. P. de Leon, J. Feist, A. V. Akimov, M. Gullans, A. S. Zibrov, V. Vuletić, and M. D. Lukin, *Science* **340**, 1202 (2013).
- ¹⁶C. J. Hood, T. W. Lynn, A. C. Doherty, A. S. Parkins, and H. J. Kimble, *Science* **287**, 1447 (2000).

- ¹⁷A. Kubanek, M. Koch, C. Sames, A. Ourjoumtsev, T. Wilk, P. W. H. Pinkse, and G. Rempe, *Appl. Phys. B* **102**, 433 (2011).
- ¹⁸T. Fischer, P. Maunz, P. W. H. Pinkse, T. Puppe, and G. Rempe, *Phys. Rev. Lett.* **88**, 163002 (2002).
- ¹⁹A. Kubanek, M. Koch, C. Sames, A. Ourjoumtsev, P. W. H. Pinkse, K. Murr, and G. Rempe, *Nature* **462**, 898 (2009).
- ²⁰T. Puppe, P. Maunz, T. Fischer, P. W. H. Pinkse, and G. Rempe, *Phys. Scr.* **T112**, 7 (2004).
- ²¹P. F. Zhang, Y. Q. Guo, Z. H. Li, Y. C. Zhang, Y. F. Zhang, J. J. Du, G. Li, J. M. Wang, and T. C. Zhang, *Phys. Rev. A* **83**, 031804(R) (2011).
- ²²P. F. Zhang, Y. C. Zhang, G. Li, J. J. Du, Y. F. Zhang, Y. Q. Guo, J. M. Wang, T. C. Zhang, and W. D. Li, *Chin. Phys. Lett.* **28**, 044203 (2011).
- ²³Y. C. Zhang, Ph.D. dissertation, Shanxi University, Tai Yuan, 2010.
- ²⁴J. J. Du, W. F. Li, P. F. Zhang, G. Li, J. M. Wang, and T. C. Zhang, *Front Phys.* **7**, 435 (2012).
- ²⁵J. Kim, M. Lee, D. Kim, W. Seo, H.-G. Hong, Y. Song, and K. An, *Opt. Lett.* **37**, 1457 (2012).
- ²⁶H. Mabuchi, Ph.D. dissertation, California Institute of Technology, California, 1997.
- ²⁷T. W. Lynn, K. Birnbaum, and H. J. Kimble, *J. Opt. B* **7**, S215 (2005).